Tunable dichroism and optical absorption of graphene by strain engineering

M. Oliva-Leyva* and Gerardo G. Naumis†
Departamento de Física-Química, Instituto de Física,
Universidad Nacional Autónoma de México (UNAM),
Apartado Postal 20-364, 01000 México, Distrito Federal, México

We theoretically study the transmittance for normal incidence of linearly polarized light between two media separated by a strained graphene monolayer. We analytically characterize the degree of dichroism and the transparency of graphene as a function of an arbitrary uniform strain and the incident polarization. We discuss how measurements of dichroism and transparency for two different polarization directions can be used to determine the magnitude and direction of strain. Ours findings result in very useful tools to tune the graphene absorption by mechanical strain, as well as to design nano devices to determine crack propagation in materials.

arXiv:1411.1376v1 [cond-mat.mes-hall] 5 Nov 2014

Strain engineering has been widely used as an effective tool to improve the technological functionality of graphene. Its electrical, chemical and optical properties are highly sensitive to mechanical deformation because of a unusual interval of elastic response. Graphene can withstand a reversible stretching up to 20%.[1]

Due to its relevance for graphene-based electronics, the band-gap opening in graphene is among the most investigated implications induced by deformations. Even though a uniaxial strain can be used to achieve the gap opening,[2,3] theoretical studies have predicted that a combination of strains results in more accessible set-ups.[4] Moreover, nonuniform deformations induce striking Landau levels due to effective pseudo-magnetic fields.[5–8] Perfect graphene has a low piezoresistive sensitivity, however, the graphene-based strain sensors are a promising field in nanotechnology.[9–11] In nano- and microelectromechanical systems, the Casimir interaction is a unwanted problem. In recent study, it was theoretically investigated how the strain modifies the force Casimir in graphene-based systems.[12] On the other hand, a simple approach has been reported to control the chemical reactivity of graphene[13]. The application of strain, via stretching of the supporting flexible substrate, produces impressive increases in the rate of reactivity.[13]

Otherwise, the concept of strain engineering has been experimentally extended to the optical domain in recent works.[14,15] Unstrained graphene (undoped) has a transparency of around 97.7% over a broad band of frequencies.[16] The origin of this remarkable feature, defined by fundamental constants, is ultimately a consequence of graphene's unique electronic structure. Needless to say, another strain effect is the anisotropy in the electronic dynamics,[17,18] which is traduced in an anisotropic optical conductivity.[19,20] Such effect for strained graphene yields a modulation of the transmittance as a function of the polarization direction. From a theoretical viewpoint, this modulation of the transmittance has been only quantified in the case of a uniaxial strain.[21] However, nowadays there are novel methods for applying biaxial strain in a controlled manner, even without the need for bending the substrate.[22] So, a more general theoretical characterization of the strained-graphene transparency is needed.

In this Letter, we quantify the modulation of the transmittance for graphene under an arbitrary uniform strain (e.g., uniaxial, biaxial, and so forth), as a function of the polarization direction. Also, we characterize the degree of polarization rotation as a function of strain and polarization direction. These results are useful to tune in effective manner the optical absorption of graphene, and hence, can be potentially utilized towards novel optical detectors, sensors, and photovoltaics.

We concentrate on the transmittance for normal incidence of linearly polarized light between two media separated by a graphene sheet which is uniformly strained, as shown in Fig. 1(a). We assume that the media are characterized by the electrical permittivities $\epsilon_{1,2}$ and the magnetic permeabilities $\mu_{1,2}$. From Fig. 1(b), we observe that the electric (E) and magnetic (H) fields belong to the graphene plane while the incident and transmitted polarizations $\theta_{i,t}$ are measured with respect to the laboratory axes xy.

For this scattering problem, one can set down immediately the boundary conditions for the electromagnetic fields, which can be written as,[23]

$$\boldsymbol{E}_t - \boldsymbol{E}_i - \boldsymbol{E}_r = 0, \tag{1}$$

$$\boldsymbol{n} \times (\boldsymbol{H}_t - \boldsymbol{H}_i - \boldsymbol{H}_r) = \boldsymbol{J}, \tag{2}$$

where $\boldsymbol{J}$ is the surface current density and $\boldsymbol{n} = (0, 0, 1)$. The electrical and magnetic field on each media are related by

$$\boldsymbol{H} = \sqrt{\frac{\epsilon}{\mu}} \frac{\boldsymbol{k} \times \boldsymbol{E}}{k}, \tag{3}$$

whereas Ohm's law reads

$$\boldsymbol{J} = \bar{\boldsymbol{\sigma}}(\omega) \cdot \boldsymbol{E}_t, \tag{4}$$

with $\bar{\boldsymbol{\sigma}}(\omega)$ being the frequency-dependent conductivity tensor of graphene. Under uniform strain, $\bar{\boldsymbol{\sigma}}(\omega)$ is given by[19,20]

$$\bar{\boldsymbol{\sigma}}(w) = \sigma_0(w)(\bar{\boldsymbol{I}} - 2\tilde{\beta}\bar{\boldsymbol{\epsilon}} + \tilde{\beta}\mathrm{Tr}\bar{\boldsymbol{\epsilon}}\bar{\boldsymbol{I}}), \tag{5}$$

where $\bar{\boldsymbol{I}}$ is the 2×2 identity matrix, $\sigma_0(w)$ is the conductivity of unstrained graphene, $\bar{\boldsymbol{\epsilon}}$ is the strain tensor and

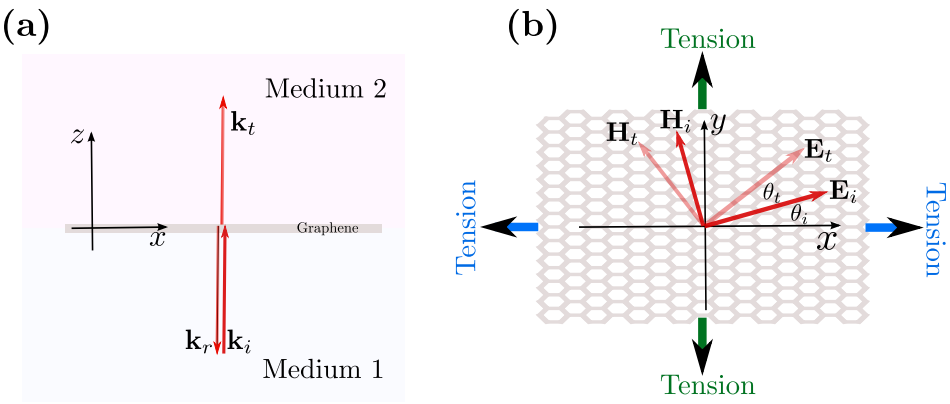

FIG. 1. (a) Front view of the scattering geometry for normal incidence between two media with strained graphene separating them. (b) Schematic representation of strain-induced dichroism as seen from above the graphene sheet. The electromagnetic fields lie in graphene plane.

$\tilde{\beta} \simeq 2.37$ is related to Grüneisen parameter. It is easy to see that an isotropic strain, $\bar{\boldsymbol{\epsilon}} = \epsilon \bar{\boldsymbol{I}}$, does not affect the conductivity whereas an anisotropic strain yields an anisotropic conductivity.

Combining Eqs. (1)-(4), we obtain

$$\boldsymbol{E}_i = \frac{1}{2}\sqrt{\frac{\mu_1}{\epsilon_1}}\left(\left(\sqrt{\frac{\epsilon_1}{\mu_1}} + \sqrt{\frac{\epsilon_2}{\mu_2}}\right)\bar{\boldsymbol{I}} + \bar{\boldsymbol{\sigma}}\right)\cdot \boldsymbol{E}_t. \quad (6)$$

Eqs. (5) and (6) shows how the strain-induced asymmetry of the conductivity tensor results in certain degree of dichroism.[21] Note that only for an isotropic conductivity (isotropic strain) the vectors $\boldsymbol{E}_i$ and $\boldsymbol{E}_t$ are collinear and then the dichroism disappears.

Now from Eq. (6) it is straightforward to write the transmittance as

$$T(\theta_i) \approx T_0\left(1 - \frac{2\sqrt{\mu_1\mu_2}}{\sqrt{\epsilon_1\mu_2} + \sqrt{\epsilon_2\mu_1}}\boldsymbol{e}_i \cdot \mathrm{Re}\bar{\boldsymbol{\sigma}} \cdot \boldsymbol{e}_i\right), \quad (7)$$

where $\boldsymbol{e}_i = (\cos\theta_i, \sin\theta_i)$ and T_0 is the transmittance for normal incidence between two media in absence of the graphene interface. The term, $\boldsymbol{e}_i \cdot \mathrm{Re}\bar{\boldsymbol{\sigma}} \cdot \boldsymbol{e}_i = \mathrm{Re}[\bar{\sigma}_{xx}\cos^2\theta_i + \bar{\sigma}_{yy}\sin^2\theta_i + \bar{\sigma}_{xy}\sin 2\theta_i]$, shows how an anisotropic absorbance yields the periodic modulation of the transmittance as a function of the polarization direction θ_i.

In order to illustrate such effects, dichroism and modulation of $T(\theta_i)$, let us assume both media to be vacuum and that the graphene is at half filling. In this case, for infrared and visible frequencies, $\sigma_0(w)$ is frequency-independent and is given by the universal value $e^2/(4\hbar)$. As a consequence, from Eqs.(5)-(7) we obtain that the polarization angles $\theta_{i,t}$ are related by

$$\theta_t - \theta_i \approx \alpha\tilde{\beta}\Big(\frac{\bar{\epsilon}_{yy} - \bar{\epsilon}_{xx}}{2}\sin 2\theta_i + \bar{\epsilon}_{xy}\cos 2\theta_i\Big)180°, \quad (8)$$

whereas the transmittance results in,

$$T(\theta_i) \approx 1 - \pi\alpha\big(1 - \tilde{\beta}(\bar{\epsilon}_{xx} - \bar{\epsilon}_{yy})\cos 2\theta_i - 2\tilde{\beta}\bar{\epsilon}_{xy}\sin 2\theta_i\big), \quad (9)$$

where α is the the fine-structure constant. Now it is easy to see the periodic modulations of the dichroism and transmittance, with a period of 180°, which is a simple consequence of the physical equivalence between the polarization angles θ_i and $\theta_i + 180°$ for normal incidence of linearly polarized light.

Let us explore first, the consequences on dichroism. In Fig. 2(a), we present the difference $\theta_t - \theta_i$ for two different deformations: a uniaxial deformation and a uniaxial-shear deformation. The resulting modulations are out of phase with each other because the principal strain directions of both deformations do not match. For the uniaxial case considered, the principal strain directions match the laboratory axes xy, and $\theta_t - \theta_i$ displays a $\sin 2\theta_i$-like modulation (see blue line). On the other hand, for the uniaxial-shear case, its principal strain directions do not

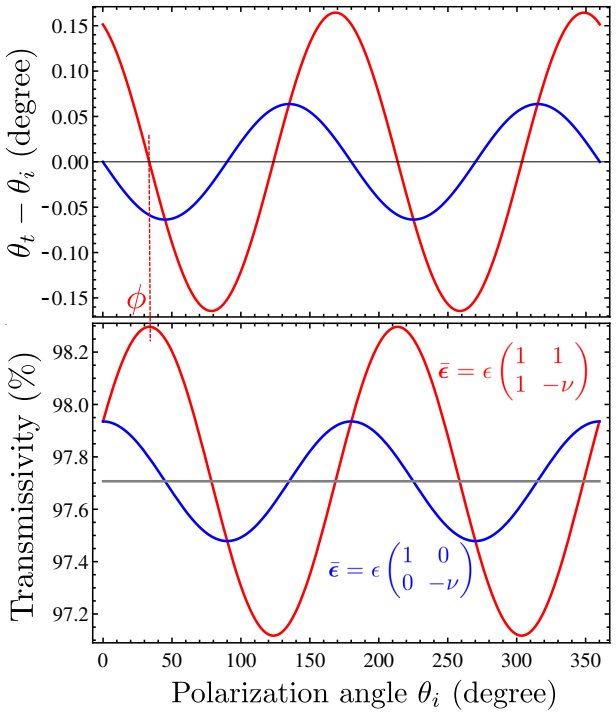

FIG. 2. Degree of dichroism (top panel) and transmittance (bottom panel) as a function of the incident polarization angle for two different deformations. The blue curves correspond to a uniaxial strain while the red curves, to a uniaxial-shear strain. We assume $\epsilon = 0.05$ for both deformations.

match the laboratory axes xy, and thus $\theta_t - \theta_i$ results in a $\sim \sin(2\theta_i - \phi)$-like modulation (see red line), with $\tan\phi = 2\bar{\epsilon}_{xy}/(\bar{\epsilon}_{xx} - \bar{\epsilon}_{yy})$. This behavior shows that the principal strain directions can be determined by measuring the polarization angles θ_i for which the incident and transmitted polarizations coincide. It is important to note that the polarization angles can be routinely measured with a precision of 0.001°, so that the predicted modulation obtained from Eq. (8) can be experimentally monitored.

Finally, let us made some important remarks about our formula (9) concerning transmittance. First of all, one can see that Eq. (9) reduces to the universal value $1 - \pi\alpha \approx 97.7\%$, which is the transmittance of unstrained or isotropically strained graphene.[16] Likewise, Eq. (9) reproduces the previously reported modulation, $1 - \pi\alpha(1 - \tilde{\beta}(1+\nu)\epsilon\cos 2\theta_i)$, for the case of a uniaxial strain along the x-axis, where ϵ is the strain magnitude and ν is the Poisson ratio ($\nu \approx 0.16$). In recent experiments, this periodic modulation of the transmittance for graphene has been confirmed.[14] In this experimental study, the strain magnitude ϵ was estimated from the modulation amplitude measurements by means of $\epsilon \approx \triangle T/(2\pi\tilde{\beta}(1+\nu))$ and confirmed from the Raman spectroscopy measurements.[14]

Thus, our Eq. (9) contains all previously studied limiting cases. Moreover, it can be used in the more general scenario of biaxial strain. In fact, it provides a simple and reliable protocol to reconstruct the principal axes of the strain tensor. The protocol goes as follows,

1) measure the transmittance at $\theta_i = 0°$,

2) measure the transmittance at $\theta_i = 45°$,

3) from Eq. (9),

$$\tan\phi = \frac{1 - \pi\alpha - T(45°)}{1 - \pi\alpha - T(0°)} \tag{10}$$

4) then ϕ is just the angle between the laboratory axes xy and the principal strain directions.

In conclusion, we calculated the dichroism and the transparency for normal incidence of linearly polarized light between two media separated by a graphene monolayer under any arbitrary uniform strain. Our results contained some previously found particular cases. Then we proposed a new protocol based in two simple transmittance measures to reconstruct the applied strain field, and in particular, the principal axes of strain. Such protocol can be extremely useful to produce nano-sensors capable to detect the local principal axis of strain, which are in fact determinant to determine crack propagation in different kind of materials. Also, it can serve to measure pseudo-magnetic fields associated with graphene.

We thank the DGAPA-UNAM project IN-102513. M. Oliva-Leyva acknowledges a scholarship from CONACyT (Mexico).

* moliva@fisica.unam.mx
† naumis@fisica.unam.mx

[1] C. Lee, X. Wei, J. W. Kysar, and J. Hone, Science **321**, 385 (2008)
[2] V. M. Pereira, A. H. Castro Neto, and N. M. R. Peres, Phys. Rev. B **80**, 045401 (2009)
[3] Z. H. Ni, T. Yu, Y. H. Lu, Y. Y. Wang, Y. P. Feng, and Z. X. Shen, ACS Nano **2**, 2301 (2008)
[4] G. Cocco, E. Cadelano, and L. Colombo, Phys. Rev. B **81**, 241412 (2010)
[5] F. Guinea, M. I. Katsnelson, and A. K. Geim, Nat Phys **6**, 30 (2010)
[6] N. Levy, S. A. Burke, K. L. Meaker, M. Panlasigui, A. Zettl, F. Guinea, A. H. C. Neto, and M. F. Crommie **329**, 544 (2010)
[7] J. V. Sloan, A. A. P. Sanjuan, Z. Wang, C. Horvath, and S. Barraza-Lopez, Phys. Rev. B **87**, 155436 (2013)
[8] Z. Qi, A. L. Kitt, H. S. Park, V. M. Pereira, D. K. Campbell, and A. H. Castro Neto, Phys. Rev. B **90**, 125419 (2014)
[9] S.-H. Bae, Y. Lee, B. K. Sharma, H.-J. Lee, J.-H. Kim, and J.-H. Ahn, Carbon **51**, 236 (2013)
[10] S.-E. Zhu, M. Krishna Ghatkesar, C. Zhang, and G. C. A. M. Janssen, Applied Physics Letters **102**, (2013)
[11] Z. Jing, Z. Guang-Yu, and S. Dong-Xia, Chinese Physics B **22**, 057701 (2013)
[12] A. D. Phan and T.-L. Phan, physica status solidi (RRL) Rapid Research Letters **9999**, n/a (2014)
[13] M. A. Bissett, S. Konabe, S. Okada, M. Tsuji, and H. Ago, ACS Nano **7**, 10335 (2013)
[14] G.-X. Ni, H.-Z. Yang, W. Ji, S.-J. Baeck, C.-T. Toh, J.-H. Ahn, V. M. Pereira, and B. Özyilmaz, Advanced Materials **26**, 1081 (2014)
[15] B. Dong, P. Wang, Z.-B. Liu, X.-D. Chen, W.-S. Jiang, W. Xin, F. Xing, and J.-G. Tian, Nanotechnology **25**, 455707 (2014)
[16] R. R. Nair, P. Blake, A. N. Grigorenko, K. S. Novoselov, T. J. Booth, T. Stauber, N. M. R. Peres, and A. K. Geim, Science **320**, 1308 (2008)
[17] M. Oliva-Leyva and G. G. Naumis, Phys. Rev. B **88**, 085430 (2013)
[18] M. Oliva-Leyva and G. G. Naumis, arXiv:1404.2619v2
[19] M. Oliva-Leyva and G. G. Naumis, Journal of Physics: Condensed Matter **26**, 125302 (2014)
[20] M. Oliva-Leyva and G. G. Naumis, Journal of Physics: Condensed Matter **26**, 279501 (2014)
[21] V. M. Pereira, R. M. Ribeiro, N. M. R. Peres, and A. H. Castro Neto, EPL **92**, 67001 (2010)
[22] H. Shioya, M. F. Craciun, S. Russo, M. Yamamoto, and S. Tarucha, Nano Letters **14**, 1158 (2014)
[23] J. D. Jackson, *Classical Electrodynamics*, 3rd ed. (Wiley, New York, 1999) p. 16